Cerebral Cortex, November 2016;26: 3828–3837

doi:10.1093/cercor/bhv180
Advance Access Publication Date: 12 August 2015
Original Article

ORIGINAL ARTICLE

Altered Human Memory Modification in the Presence of Normal Consolidation

Nitzan Censor[1,2], Ethan R. Buch[1], Karim Nader[3], and Leonardo G. Cohen[1]

[1]Human Cortical Physiology and Neurorehabilitation Section, National Institute of Neurological Disorders and Stroke, National Institutes of Health, Bethesda, MD 20892, USA, [2]School of Psychological Sciences and Sagol School of Neuroscience, Tel Aviv University, Tel Aviv 69978, Israel and [3]Department of Psychology, McGill University, Montreal, QC, Canada

Address correspondence to email: censornitzan@post.tau.ac.il

Abstract

Following initial learning, the memory is stabilized by consolidation mechanisms, and subsequent modification of memory strength occurs via reconsolidation. Yet, it is not clear whether consolidation and memory modification are the same or different systems-level processes. Here, we report disrupted memory modification in the presence of normal consolidation of human motor memories, which relate to differences in lesioned brain structure after stroke. Furthermore, this behavioral dissociation was associated with macrostructural network architecture revealed by a graph-theoretical approach, and with white-matter microstructural integrity measured by diffusion-weighted MRI. Altered macrostructural network architecture and microstructural integrity of white-matter underlying critical nodes of the related network predicted disrupted memory modification. To the best of our knowledge, this provides the first evidence of mechanistic differences between consolidation, and subsequent memory modification through reconsolidation, in human procedural learning. These findings enable better understanding of these memory processes, which may guide interventional strategies to enhance brain function and resulting behavior.

Key words: diffusion, DWI, MRI, procedural memory consolidation, sequence learning, reconsolidation

Introduction

Once formed and stabilized through consolidation (Glickman 1961; Kandel 2001), memories are dynamic and change over time. Following their reactivation or retrieval (Alberini 2011; Nader and Hardt 2009), previously consolidated memories return to a labile form, which can be substantially modified (enhanced, maintained, updated, or degraded) (Lee 2008; Monfils et al. 2009). Accordingly, the memory must undergo reconsolidation following its reactivation, or else may be lost (Nader and Hardt 2009; Alberini 2011). Following memory reactivation, both cellular-level (Nader et al. 2000; Lee et al. 2004; Alberini 2011) and systems-level memory reconsolidation (Debiec et al. 2002; Sandrini et al. 2013; Censor, Dayan et al. 2014, Censor, Horovitz et al. 2014) may enable additional learning with repetitive training sessions leading to strengthening of memories, crucial for daily life (Lee 2008). At the systems level, interference with reactivation using behavioral or noninvasive brain stimulation paradigms was shown to alter reconsolidation of the memory (Walker et al. 2003; Censor et al. 2010; de Beukelaar et al. 2014). Thus, in the absence of interference, memory modification through reconsolidation may result in strengthening of the memory, expressed as improved performance measured on the following day (Walker et al. 2003; Censor et al. 2010; de Beukelaar et al. 2014). Consistently, it has been shown in rodents that memory reconsolidation mediates memory strengthening by additional learning (Lee 2008). Thus overall, while encoded memories are transformed into long-term memory through consolidation, reactivation of previously consolidated memories can result in memory strengthening. However, while representing different

stages of memory formation, it is not clear whether memory consolidation and subsequent memory modification through reconsolidation represent the same or different systems-level mechanistic processes and if they are sustained by the same or different structural substrates. Here, we report for the first time a dissociation between intact consolidation and impaired memory modification in human procedural learning.

Since procedural learning engages extensive networks of spatially remote brain regions (Dayan and Cohen 2011), a valuable strategy to explore structural substrates of consolidation and reconsolidation would be to study pathological conditions in which different nodes within these distributed networks are lesioned. Thus, the purpose of the study was to identify whether lesions altering structural brain networks underlie dissociable behavioral manifestations of consolidation and reconsolidation. Previous studies in motor learning have suggested that while prefrontal executive and attentional resources are more involved in early learning stages that may be followed by consolidation processes, fine-tuning of the motor memory is enabled by core regions of the motor network, which is primarily located in frontoparietal cortical areas and the subcortical sensorimotor striatum (Hikosaka et al. 2002; Ungerleider et al. 2002; Dayan and Cohen 2011), which may support subsequent reconsolidation processes (Censor, Dayan et al. 2014; Censor, Horovitz et al. 2014). To that effect, patients with chronic stroke involving motor impairments resulting from cortical and subcortical lesions affecting the motor network (see Fig. 1, and Supplementary Table 1), and healthy aged-matched controls, carried out an experimental learning task requiring acquisition and consolidation of a sequence of finger movements (Karni et al. 1995; Walker et al. 2003; Censor et al. 2010; de Beukelaar et al. 2014). We proposed that structural impairments in this motor network might differentially impact consolidation and reconsolidation. Patients and healthy controls were tested on 3 separate days, with performance measured as the number of correct sequences during each 30-s trial (see Materials and Methods). Trials were identical on all days. On Day 1, performance was tested immediately after training. On Day 2, all participants performed test trials to measure offline consolidation following Day 1 (from Day 1 to Day 2) and to reactivate the originally trained memory (Walker et al. 2003; Lee 2008; Censor et al. 2010; de Beukelaar et al. 2014). On Day 3, all participants performed only retest trials to evaluate offline modification of memory strength through reconsolidation following Day 2 reactivation (from Day 2 to Day 3) (Walker et al. 2003; Censor et al. 2010; de Beukelaar et al. 2014). First, the patients show a behavioral dissociation between intact consolidation and impaired memory modification. Then, the behavioral outcomes were related to structural network architecture using a graph-theoretical network analysis approach (Rubinov and Sporns 2010; Zhang et al. 2010; see Materials and Methods), and to local white-matter (WM) microstructural integrity using diffusion-weighted MRI (Mori and Zhang 2006; see Materials and Methods). Impaired memory modification, in the presence of normal consolidation, is associated with altered brain network architecture and microstructural integrity of WM underlying critical nodes of the related network. These results document a system-level dissociation between memory consolidation and memory modification through reconsolidation.

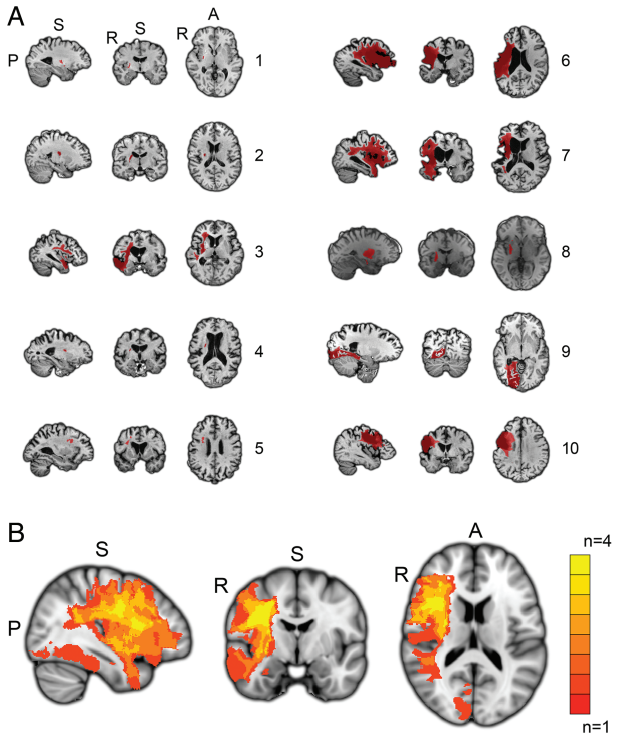

Figure 1. Individual patient MRI data. (*A*) Sagittal, coronal, and axial views of individual patients' T1-weighted MRI scans with segmented brain lesions. Slices for each view are shown at the center-of-gravity location for the lesion. (*B*) Group lesion probability maps displayed in MNI152 space (slices through MNI coordinate: $X = 38$, $Y = -5$, $Z = 15$). Lesion aligned to the left hemisphere. The map shows voxels where at least 1 patient has a lesion (red), and up to 4 (yellow).

Materials and Methods

Subjects

Ten naïve chronic stroke patients (age mean 62.6 ± 9.1 standard deviation) and 10 naïve aged-matched right-handed healthy subjects (age mean 60.4 ± 8.1 standard deviation) participated in the study. All participants gave written informed consent. Work was done under approval of the Combined Neuroscience Institutional Review Board of the National Institutes of Health, and deviations in the number of sessions performed and their precise timing were reported to the Institutional Review Board. Participation in the study required reporting at least 6 h of sleep the night before each experimental session, not being an active musician, and ability to perform and learn the motor task (Censor et al. 2010). Patients' inclusion criteria were stroke involving motor deficits with onset of >6 months and Folstein Mini-Mental State Examination (Folstein et al. 1975) scores of >23 out of 30.

Task

Participants performed a sequential finger-tapping task (Walker et al. 2003; Korman et al. 2007; Censor et al. 2010; de Beukelaar et al. 2014), used before to characterize reconsolidation of previously consolidated motor memories in humans in different laboratories (Walker et al. 2003; Censor et al. 2010; de Beukelaar et al. 2014). Each trial lasted for 30 s, in which participants had to repeatedly tap with their stroke-affected (patients, see Supplementary Table 1) or left (Walker et al. 2003; Korman et al. 2007; Censor et al. 2010) (healthy controls) hand as quickly and accurately as possible a sequence of finger movements (4-1-3-2-4) using a 4-key response pad. Feedback was given, with each key press producing a dot on the screen and with dots forming a row from left to right as the trial progressed. Each trial was

followed by a 30-s break until the next trial started. As in previous studies (Censor et al. 2010), the number of correct sequences performed during each fixed 30-s trial was the primary outcome measure.

Experimental Procedure

All participants (patients and healthy controls) took part in 3 daily sessions. Trials were identical on all days. On Day 1, participants performed 9 training trials followed immediately afterward by 3 post-training trials. On Day 2, participants performed 3 test trials to measure consolidation from Day 1 to Day 2 and to reactivate the originally trained memory (Walker et al. 2003; Censor et al. 2010; de Beukelaar et al. 2014). On Day 3, participants performed 3 retest trials to evaluate memory modification through reconsolidation. All sessions were performed before 3 p.m., with participants instructed to continue their usual daily routine.

Control experiments: To determine the extent of normal consolidation after a delay (without reactivation), on Day 1 participants (the patients and the healthy controls) performed 9 training trials with a novel sequence (4-2-3-1-4, thus they were not familiarized with this sequence in the main experiment) (Karni et al. 1995) followed immediately afterward by 3 post-training trials. On Day 3, participants performed 3 test trials to evaluate memory consolidation after a delay. Of note, control experiments were performed separately from the main experiment in order to avoid interference effects (all control experiments were performed at least a month after the main experiment). Patients continued to perform the same sequence for multiple days in order to evaluate performance-ceiling effects (Day 3, 12 additional trials; Day 4, 15 trials; Day 5, 3 final trials). To determine the specificity of the learning effects to the trained sequence, patients were additionally tested on Day 3 with 3 trials of an untrained sequence (2-3-1-4-2, compared with Day 1 post-training of the original sequence) (Walker et al. 2003). Of note, these 3 trials were performed before the additional 12 trials of the original sequence on Day 3 to avoid anterograde interference effects.

Imaging Data Acquisition

Whole-brain, single-shot echo-planar (EPI) diffusion-weighted volumes (110 noncollinear directions; b = 100 [10 volumes], 300 [10], 500 [10], 800 [30] or 1100 s mm^{-2} [50]; 60 slices; voxel size 2.5 × 2.5 × 2.5 mm^3; TE/TR = 76.4 ms/18.28 s) plus 10 volumes without diffusion weighting (b = 0 s mm^{-2}) were acquired for patients on a 3.0 Tesla GE Excite HDxt scanner using an 8-channel coil (GE Medical Systems,). In addition, structural T_1-weighted (MPRAGE sequence; TE/TR = 2.67 ms/6.26 s, flip angle = 12°; voxel size = 0.9375 × 0.9375 × 1 mm^3) and T_2-weighted (TE/TR = 122.52 ms/8.35 s; voxel size = 0.4688 × 0.4688 × 1.5 mm^3) volumes were acquired.

Behavioral Data Analysis

The performance outcome measure was the number of correct sequences achieved per each 30-s trial, an endpoint measure in which memory reconsolidation has proven consistent and reproducible within and across laboratories (Walker et al. 2003; Censor et al. 2010; de Beukelaar et al. 2014). For each participant, performance was averaged over the post-training trials and each set of test and retest trials. To exclude potential warm-up decrements and fatigue, in all groups the 2 best trials from each day were taken as endpoint measures for session performance, consistent with previous studies (Celnik et al. 2009). Comparisons were performed with repeated-measures analysis of variance (ANOVA, following baseline normalization of each participant's performance relative to Day 1 post-training performance) and paired (within-group) or unpaired (between group) *t* tests with the Bonferroni correction for multiple comparisons.

MRI Data Analysis

Preprocessing of the DWIs was performed with algorithms included in the TORTOISE software package (www.tortoisedti.org) (Pierpaoli et al. 2010). DWIs were first corrected for motion and eddy current distortions including proper re-orientation of the b-matrix to account for the rotational component of the subject rigid-body motion (Rohde et al. 2004; Leemans and Jones 2009). In addition, B0 susceptibility induced EPI distortions were corrected using an image registration-based approach using B-Splines (Wu et al. 2008). All corrections were performed in the native space of the DWI images. For consistency, all images were reoriented into a common space defined by the mid-sagittal plane, the anterior, and the posterior commissure (Bazin et al. 2007) also with appropriate rotations to the b-matrix. A nonlinear diffusion tensor model was then fit to the corrected data. Tensor volumes for patients with left-hemispheric lesions were then left-right flipped, with appropriate reflections of the tensors applied as well. Following tensor estimation, spatial normalization was performed using a nonparametric, diffeomorphic deformable image registration technique implemented in DTI-TK (www.nitrc.org/projects/dtitk/) that incrementally estimates its displacement field using a tensor-based registration formulation (Zhang et al. 2006). It is designed to take advantage of similarity measures comparing tensors as a whole via explicit optimization of tensor reorientation and includes appropriate reorientation of the tensors following deformation.

Lesion segmentation: Lesions in each patient were segmented using an iterative, partially unsupervised method. First, T_2-weighted volumes were rigid-body aligned with T_1-weighted volumes. These 2 aligned volumes were then used as multichannel inputs to the FMRIB Automated Segmentation Tool (FAST), a part of the FMRIB Software Library (FSL; http://www.fmrib.ox.ac.uk/fsl/). FAST was used to derive partial volume estimates (PVEs) at each voxel for gray matter (GM), WM, and cerebral spinal fluid (CSF) tissue classes. These PVEs were then nonlinearly transformed into MNI152 space using FNIRT, and compared with a custom reference healthy brain atlas of PVEs through the computation of a distance map (measured as the Euclidean distance between stroke patient and healthy brain template GM, WM, and CSF PVE vectors at each voxel location). The resulting distance map was thresholded at 0.95 and binarized to create a lesion mask in MNI space. An MNI-space ventricular mask was then used to remove any part of the lesion mask that included portions of the ventricles. The resulting lesion mask was then eroded, dilated, and smoothed with a 1-mm-radius spherical kernel and transformed back into the original subject space using the inverse nonlinear warp field. This subject space lesion mask was then used as an exclusion mask for the subsequent nonlinear registration iteration, resulting in a change to the nonlinear registration of the subject PVE to the MNI template. A total of 10 iterations were performed in this manner. The final lesion masks were then visually inspected and manually corrected if needed (Buch et al. 2012).

Structural Network Construction

We used the Johns Hopkins University Probabilistic Fiber Atlas (http://cmrm.med.jhmi.edu) (Zhang et al. 2010) in conjunction

with the segmented individual patient lesions to derive a structural connectivity matrix and construct a weighted, undirected structural network graph. ROIs used as seeds and targets in the construction of the atlas were employed as nodes in the anatomical network. Probabilistic atlas tracts were used to define connections between each node based on the published tractography-based connectivity matrix (Zhang et al. 2010). For each patient, lesion segmentation masks were nonlinearly transformed into the common atlas space, with all tract values for voxels overlapping with the lesion mask in a particular patient set to zero. As the probability value for each tract falls off at voxels distant from its center, this meant that lesion overlap with central regions of each tract was weighted more heavily in terms of the impact on structural connectivity. The weight for a given network connection was defined as the ratio of the spared fiber tract probability sum to the total original tract probability sum.

Since it is highly probable that the net effect of a lesion that transects an entire fiber tract is greater than an effect caused by a reduction in tract volume, we used a custom search algorithm to identify transections by labeling noncontiguous components of the tract following the zeroing of tract voxels overlapping with the lesion segmentation. If a transection resulted in multiple noncontiguous tract sections that were >20% of the overall tract volume, the connectivity weight for that tract was set to zero. The 20% threshold was used to ensure that transections were only counted if they occurred within the main body of the tract, and not if they only occurred in lower probability terminal portions near the grey/white matter border, where tractography is less reliable.

We decided against using a tractography-based approach to define our structural network as peri-infarct regions usually contain high amounts of glial cell aggregation that significantly affect water diffusion anisotropy in a complex manner (Budde and Frank 2010). Under these circumstances, the relative contribution of WM microstructure properties and gliosis to between-subject differences in measured anisotropy cannot be fully dissociated with standard diffusion MRI techniques (Newton et al. 2006; Kunimatsu et al. 2007). To avoid this confound, we implemented lesion segmentation overlaps with a probabilistic atlas of major WM fiber bundles derived from data acquired in healthy volunteers and gain insight into the disruption of structural connectivity within the ipsilesional hemisphere along with the effects on the contralesional hemisphere (Riley et al. 2011; Buch et al. 2012).

Measures of nodal betweenness centrality, which describe the degree to which individual brain regions contribute to the shortest pathway connecting other brain regions, were calculated for each patient's weighted structural connectivity matrix. The nodal betweenness centrality of a given node n is defined as follows (Buch et al. 2012):

$$C_B(n) = \sum_{i \neq n \neq j} \frac{\sigma_{ij}(n)}{\sigma_{ij}},$$

where σ_{ij} is the total number of shortest paths from node i to node j and $\sigma_{ij}(n)$ is the number of those shortest paths that pass through node n.

Tract-Based Spatial Statistics Analysis of Extralesional Fractional Anisotropy

To explore extralesional structural network characteristics, we used a complimentary tract-based spatial statistics analysis approach that characterizes WM microstructure relationships associated with memory modification in voxels not contributing to the lesion segmentation in any patient. FA maps for each patient were created from the spatially normalized tensor outputs from DTITK. A mean FA image was created and then skeletonized using an FA threshold of 0.2. Each patient's aligned FA image was then projected onto this mean skeleton by searching perpendicular from the skeleton for maximum FA values. This step allows for the statistical comparison of FA values from homologous regions of the FA map. An extralesional group mask was constructed by summing individual patient lesion masks transformed into the common group tensor space, binarizing, and then inverting. Thus, only voxels falling outside the lesion mask boundaries in all patients were included in subsequent analyses. Between-subject variance in FA of homologous regions was then related to memory modification scores. The TFCE (threshold free cluster enhancement) option, a novel method for enhancing cluster-like structures in statistical images, was used for subsequent statistical tests. Resulting false discovery rate (FDR) (Genovese et al. 2002)-corrected P-value maps were thresholded at $P \leq 0.05$. Average FA values within clusters were then correlated (Pearson's correlation) with the memory modification score to determine the correlation coefficient for the cluster.

Results

We used a behavioral paradigm that engages consolidation and reconsolidation of procedural motor sequence memories (Walker et al. 2003; Censor et al. 2010; de Beukelaar et al. 2014). Stroke patients (Supplementary Table 1) and healthy aged-matched controls were tested with the motor sequence task on 3 consecutive days, with consolidation measured as offline performance gains between Day 1 and Day 2, and memory modification through reconsolidation as performance gains between Days 2 and 3 (Walker et al. 2003; Censor et al. 2010; de Beukelaar et al. 2014) (Fig. 2A, see Materials and Methods, and Supplementary Tables 2 and 3). Following initial within-session learning (Supplementary Fig. 1), a repeated-measures ANOVA showed a significant group by day interaction ($F_{2,36} = 3.53$, $P < 0.05$). While consolidation was comparable in both groups ($P = 0.25$), patients' memory modification was significantly lower than that of healthy controls ($P < 0.02$). The patients improved performance on Day 2, showing efficient initial acquisition and consolidation (mean performance gains between Day 1 post-training and Day 2 test 25.6 ± 8.6% standard error, $P < 0.03$; Fig. 2B and C). However, memory modification following reactivation in the patient group, usually expressed as improvement in memory strength (Walker et al. 2003; Censor et al. 2010), was impaired (with no significant performance gains between Days 2 and 3, −8.9 ± 7.7%, $P = 0.45$; Fig. 2B and C). Within-group consolidation and memory modification magnitudes in the patient group were significantly different ($P < 0.03$; Fig. 2C). There were no significant differences in patients' performance between Day 1 and Day 3 ($P = 0.13$), suggesting that impaired memory modification following reactivation may have reduced the benefits of initial consolidation (Walker et al. 2003). Healthy controls showed efficient consolidation (18.3 ± 6.4%, $P < 0.02$; Fig. 2B and C) but, unlike patients, showed efficient memory modification (10.6 ± 2.6%, $P < 0.004$; Fig. 2B and C). Within-group consolidation and memory modification magnitudes were not significantly different in healthy controls ($P = 0.15$), unlike in the patient group (Fig. 2C).

To determine the stability of consolidation following a delay, the patients and healthy controls practiced in a separate experiment a sequence on Day 1 and were subsequently tested on

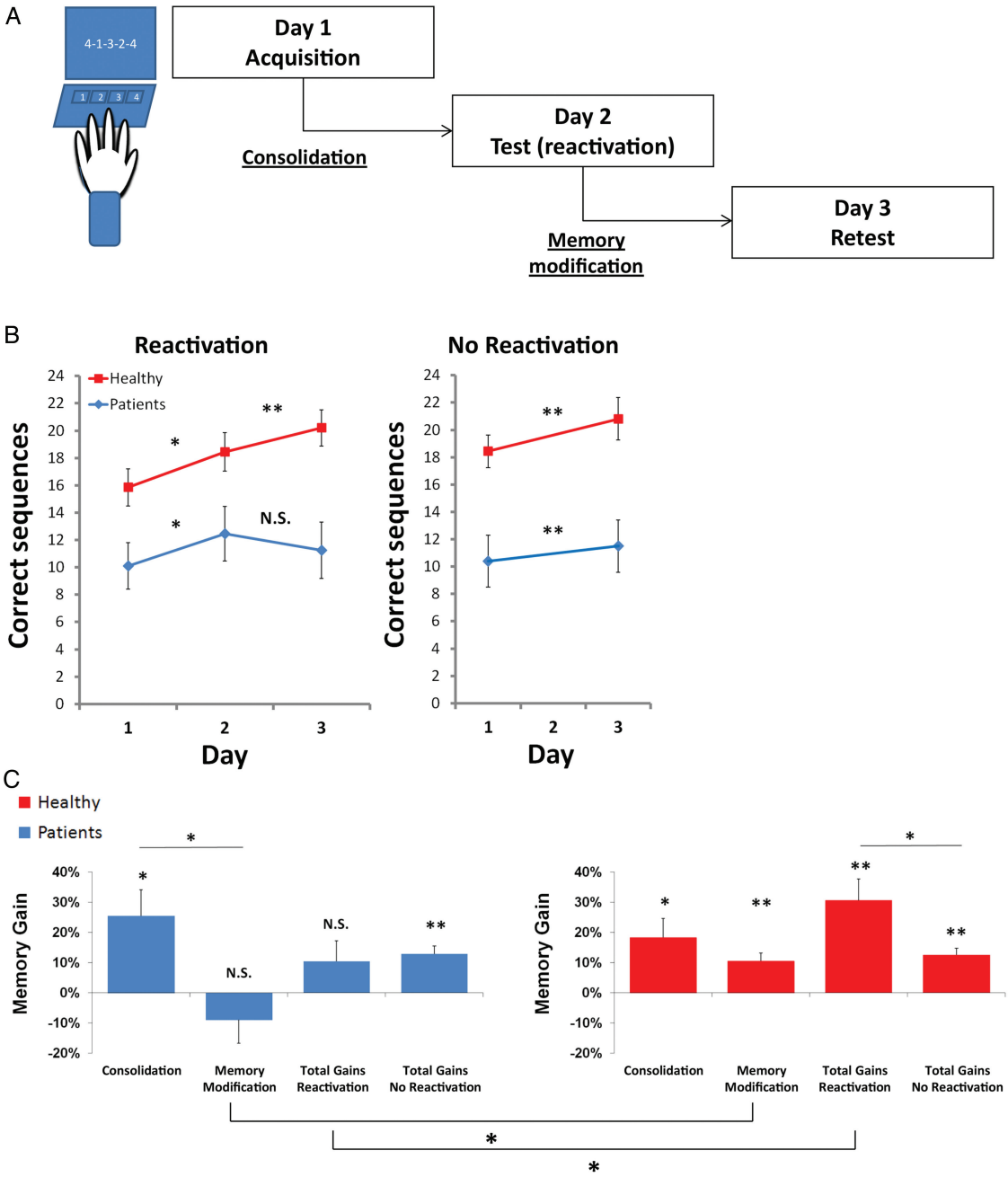

Figure 2. Experimental design and behavioral results. (*A*) Participants were trained to tap a 5-digit sequence. Intact consolidation of the memory was assessed on Day 2 as the offline memory performance gains from the end of the Day 1 session. Memory modification was assessed on Day 3 as the offline memory gains from Day 2. (*B*) Patients' ($n = 10$) and healthy aged-matched controls' ($n = 10$) learning curve across days, when the memory was reactivated on Day 2 and when it was not. (*C*) Healthy controls showed intact consolidation and memory modification. Patients showed intact consolidation but impaired memory modification, which was significantly different from their consolidation and from healthy controls' memory modification. There were significant differences in performance between Day 1 and Day 3 (Total Gains) with no reactivation in the patient group, indicating stable consolidation following a delay that was comparable with healthy controls. In the healthy control group, improvements between Day 1 and Day 3 with Day 2 reactivation were significantly greater than those without Day 2 reactivation. Thus, Day 2 reactivation enabled efficient reconsolidation that mediated memory strengthening, resulting in offline improvements in performance. Contrary to healthy controls, in the patient group, improvements between Day 1 and Day 3 with Day 2 reactivation were not significantly different from without Day 2 reactivation. Repeated-measures ANOVA and t-tests were used. Error bars express standard errors. $^{**}P < 0.005$; $^{*}P < 0.05$.

Day 3, in the absence of memory reactivation trials (see Materials and Methods). A repeated-measures ANOVA showed a significant group (Patients, Healthy controls) by condition (Reactivation, No reactivation) by day (Day 1, Day 3) interaction ($F_{1,16} = 4.82$, $P < 0.05$). Contrary to the reactivation condition reported above, in the no reactivation condition a repeated-measures ANOVA did not show a significant group by day interaction ($F_{1,16} = 0.013$, $P = 0.91$). There were significant differences in performance between Day 1 and Day 3 with no reactivation in the patient group (12.9 ± 2.6%, $P < 0.0001$) indicating stable consolidation following a delay, which was comparable ($P = 0.45$) with healthy controls (12.5 ± 2.2%, $P < 0.005$, Fig. 2*B* and *C*).

Interestingly, a repeated-measures ANOVA showed a significant group (Patients, Healthy controls) by condition (Reactivation, No reactivation) interaction ($F_{1,16} = 78.68$, $P < 0.0001$). In the healthy control group, improvements between Day 1 and Day 3 with Day 2 reactivation (30.6 ± 7.2%, $P < 0.005$) were significantly greater ($P < 0.05$) than those without Day 2 reactivation (12.5 ± 2.2%, $P < 0.005$, Fig. 2C). Thus, Day 2 reactivation enabled efficient modification of memory strength, resulting in offline improvements in performance. Contrary to healthy controls, in the patient group, improvements between Day 1 and Day 3 with Day 2 reactivation (10.4 ± 6.8%, $P = 0.13$) were not significantly different ($P = 0.36$) from those without Day 2 reactivation (12.9 ± 2.6%, $P < 0.0001$).

Of note, when the patients continued with extensive training (rather than a brief reactivation) after testing on Day 3, performance levels continued improving relative to Day 1 (61.1 ± 13.0%, $P < 0.0005$). Thus, the absence of improvements in memory could not be explained by a ceiling effect on performance. When the patients were tested on Day 3 with an untrained sequence, performance did not improve relative to Day 1 post-training ($P = 0.24$, with performance levels even lower than Day 1 by 14.0 ± 6.8%), indicating that between-session consolidation effects were specific to the trained sequence as shown in previous studies (Karni et al. 1995; Walker et al. 2003), but pointing to some transfer of learning effects since the first trials of the untrained sequence were not significantly different from the last Day 1 trials of the original sequence. In addition, a repeated-measures ANOVA testing for possible carry-over effects between the different sequences performed in the Reactivation and No reactivation experiments did not show a significant group (Patients, Healthy controls) by condition (Day 1 Reactivation, Day 1 No reactivation) interaction ($F_{1,16} = 2.90$, $P = 0.11$). As expected due to motor impairments in the patient group, there was a significant group effect ($F_{1,16} = 9.01$, $P = 0.008$). There was a marginally significant condition effect ($F_{1,16} = 4.36$, $P = 0.053$). However, within each group, the Reactivation and No-Reactivation conditions were not significantly different ($P = 0.74$ for the Patient group, $P = 0.07$ for the Healthy control group) and these nonsignificant differences between the conditions also were not significantly different between the 2 groups ($P = 0.13$). As for the initial within-session effects (Supplementary Fig. 1), a repeated-measures ANOVA with condition (Reactivation, No reactivation) and trial (9) as within-subject factors, and group (Patients, Healthy controls) as the between-subject factor showed a significant effect of condition ($F_{1,16} = 4.94$, $P = 0.04$), however did not show a significant condition by group interaction ($F_{1,16} = 1.64$, $P = 0.22$: Within the Healthy control group, there was no significant condition effect [$P = 0.10$], nor within the Patient group [$P = 0.37$]). Moreover, there was no significant

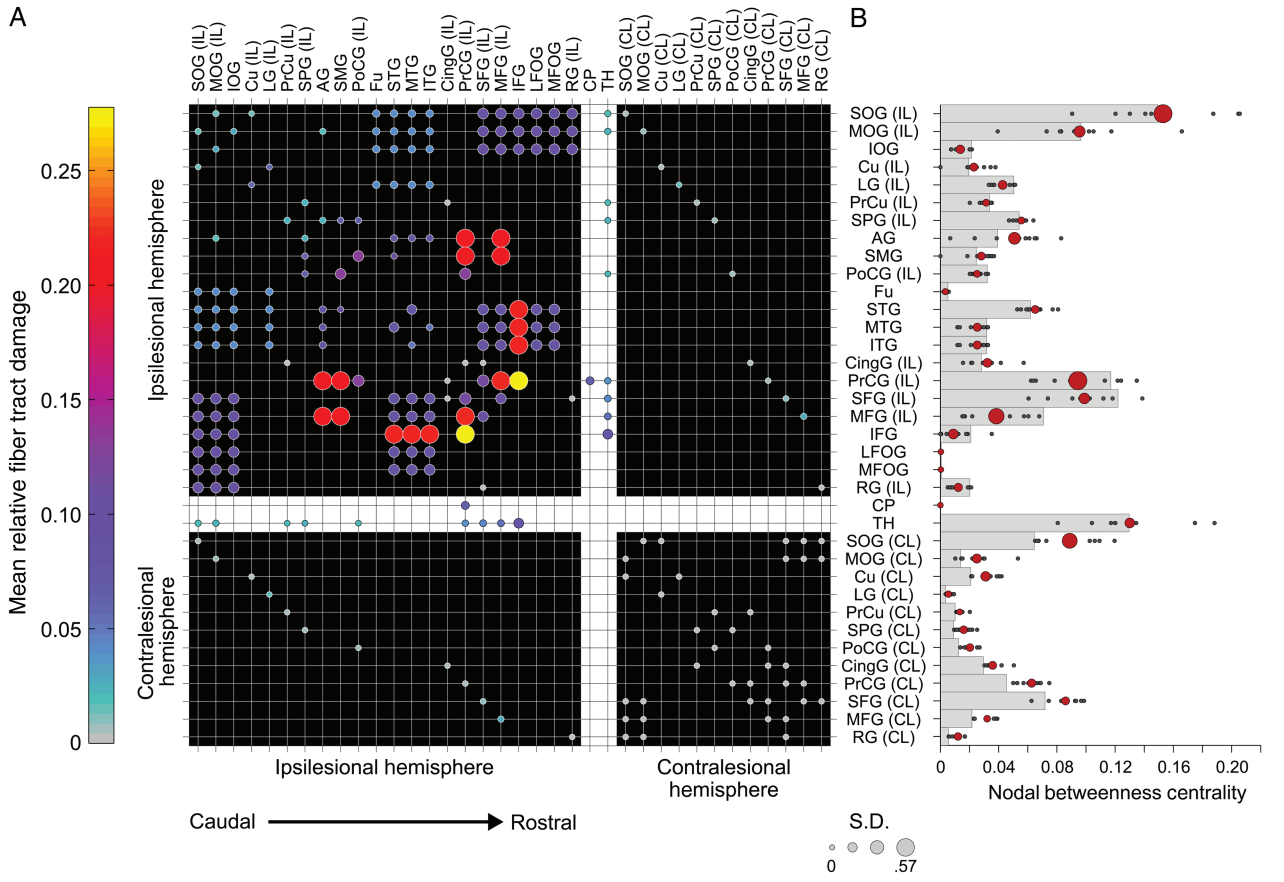

Figure 3. Structural network architecture. (*A*) WM fiber tract lesion damage. The most severe damage (marked with red and yellow) affected WM pathways involving the precentral (PrCG), the inferior (IFG), and the middle (MFG) frontal gyri network nodes. Network pathways representing ipsilesional hemisphere short and long association fibers are located in the top-left quadrant (with the black background). Transcallosal fiber pathways are located in lower-left and upper-right quadrants. Contralesional hemisphere short and long association fiber pathways between contralesional nodes directly connected to ipsilesional nodes through transcallosal pathways are located in the lower-right quadrant. Circle diameters denote standard deviation of the mean. (*B*) Contribution of each nodal brain region in the lesioned and normal networks to global structural network integration, nodal betweenness centrality. Gray bars denote the normal network. Red circles denote the mean lesioned network (diameter representing the standard deviation of the mean), with individual patient scores represented by small gray circles.

condition by trial interaction ($F_{3.64,58.23} = 0.49$, $P = 0.73$) nor a significant condition by trial by group interaction ($F_{3.64,58.23} = 2.17$, $P = 0.09$).

These results document for the first time a behavioral dissociation between intact consolidation and disrupted memory modification in procedural learning, raising the hypothesis of possible mechanistic differences.

Memory modification impairments were then related to structural network architecture using a graph-theoretical network analysis approach (Rubinov and Sporns 2010; Zhang et al. 2010), and to local WM microstructural integrity using diffusion-weighted MRI (Mori and Zhang 2006). First, structural MRI was used to segment the stroke lesions (see Materials and Methods, and Fig. 1) (Zhang et al. 2010). Using this information, we then implemented a graph-theoretical network analysis to characterize the lesioned network by evaluating the impact of lesion damage in individual patients on a normal structural brain network derived from a probabilistic atlas of WM fiber tracts previously published in healthy volunteers (Zhang et al. 2010). Network architecture differences in individual stroke patients relative to the normal brain derived from the atlas were quantified (Buch et al. 2012) (see Materials and Methods). The patients' most affected WM pathways were those connecting precentral gyrus, inferior frontal, and middle-frontal gyri nodes (Fig. 3*A*, and Supplementary Fig. 2). Specifically, these included short association fiber pathways connecting the precentral gyrus to the inferior and middle-frontal gyri, the temporal portion of the superior longitudinal fascicle (SLF) connecting the inferior frontal gyrus to the inferior middle and superior temporal gyri, and the frontoparietal portion of the SLF connecting the precentral and middle-frontal gyrus with the angular and supramarginal gyri in the posterior parietal cortex (Fig. 3*A*).

We then measured the contribution of each nodal brain region to global structural network integration, nodal betweeness centrality (Rubinov and Sporns 2010) (see Materials and Methods), which reflects the degree to which a single node in a network integrates information between all other nodal pairs (Rubinov and Sporns 2010). Brain regions showing high betweenness centrality are important for the global integration of information across the brain. This integration of distributed information could be a key network mechanism underlying learning and memory formation (Hermundstad et al. 2011; Buch et al. 2012). We used these data to relate memory modification to structural network abnormalities. Out of all network nodes (Fig. 3*B*), memory modification correlated only with the difference in nodal betweenness centrality between patients' and normals' networks in the contralesional medial-frontal gyrus (MFG, $r = 0.83$; $P < 0.005$; Fig. 4). Thus, contralesional MFG, interconnected with the ventral premotor cortex (PMv), may serve as an important hub integrating information required for efficient modification of memory strength.

We then related memory modification to extralesional WM microstructural integrity, measured as fractional anisotropy (FA) (see Materials and Methods). Memory modification correlated with FA in 3 contralesional hemisphere WM regions ($P < 0.005$): underlying the vicinity of the precentral gyrus ($X = -21$, $Y = -21$, $Z = 60$; Fig. 5*A*), the medial-frontal gyrus (MFG, −34, 18, 31; Fig. 5*B*), and the anterior intraparietal area (AIP, −46, −45, 39; Fig. 5*C*). This result further supports a link between MFG and memory strengthening via reconsolidation. Consistently, nodal betweenness centrality in the contralesional MFG correlated with FA in WM underlying the same region ($r = 0.80$, $P < 0.006$; Fig. 5*D*). It is conceivable that microstructural integrity of WM underlying the precentral gyrus, as measured by FA, relates to the role of primary motor cortex processing in motor memory modification (Censor et al. 2010).

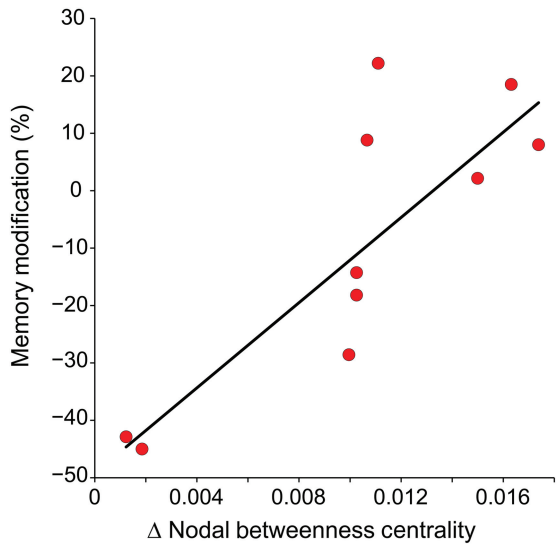

Figure 4. Relation of memory modification to structural network architecture. The difference in nodal betweenness centrality between patients' and normals' networks only in the contralesional MFG correlated positively with memory modification scores. This finding suggests that the contralesional MFG, interconnected with areas related to motor learning, is an important hub integrating information for efficient memory modification.

Contrary to memory modification, consolidation did not correlate with the difference in MFG nodal betweenness centrality between patients' and normals' networks ($P > 0.05$, significantly different from the correlation between MFG nodal betweenness centrality and memory modification, $P < 0.007$). Consolidation but not memory modification correlated negatively with FA in a single cluster in the rostral contralesional superior longitudinal fasciculus (Supplementary Fig. 3).

Discussion

All together these findings support mechanistic differences underlying consolidation, and memory modification through reconsolidation, in procedural learning. Modification of memory strength was impaired in the presence of normal consolidation and was associated with altered structural network architecture and WM microstructural integrity underlying contralesional regions homologous to the damaged WM pathways. First, with WM underlying the middle-frontal gyrus interconnected with the ventral premotor cortex, a crucial node involved in visuomotor transformations required for skilled prehension behavior (Borra et al. 2008). Second, with WM underlying the anterior intraparietal area with dense connections to motor regions adjacent to the precentral gyrus (Duque et al. 2008) and third, with WM underlying the primary motor cortex (M1), involved in bilateral hand motor control, memory formation, and memory modification (Censor et al. 2010).

Thus, the results here show that microstructural integrity of WM underlying M1, as well as the anterior intraparietal area and middle-frontal gyrus interconnected with M1 and premotor cortex, is associated with the degree of memory modification. These structural correlates suggest that consolidation and reconsolidation are supported by different substrates, explaining previous studies in which disruption of M1 processing does not impair consolidation measured the following day (Robertson et al. 2005) but did impair memory reconsolidation (Censor

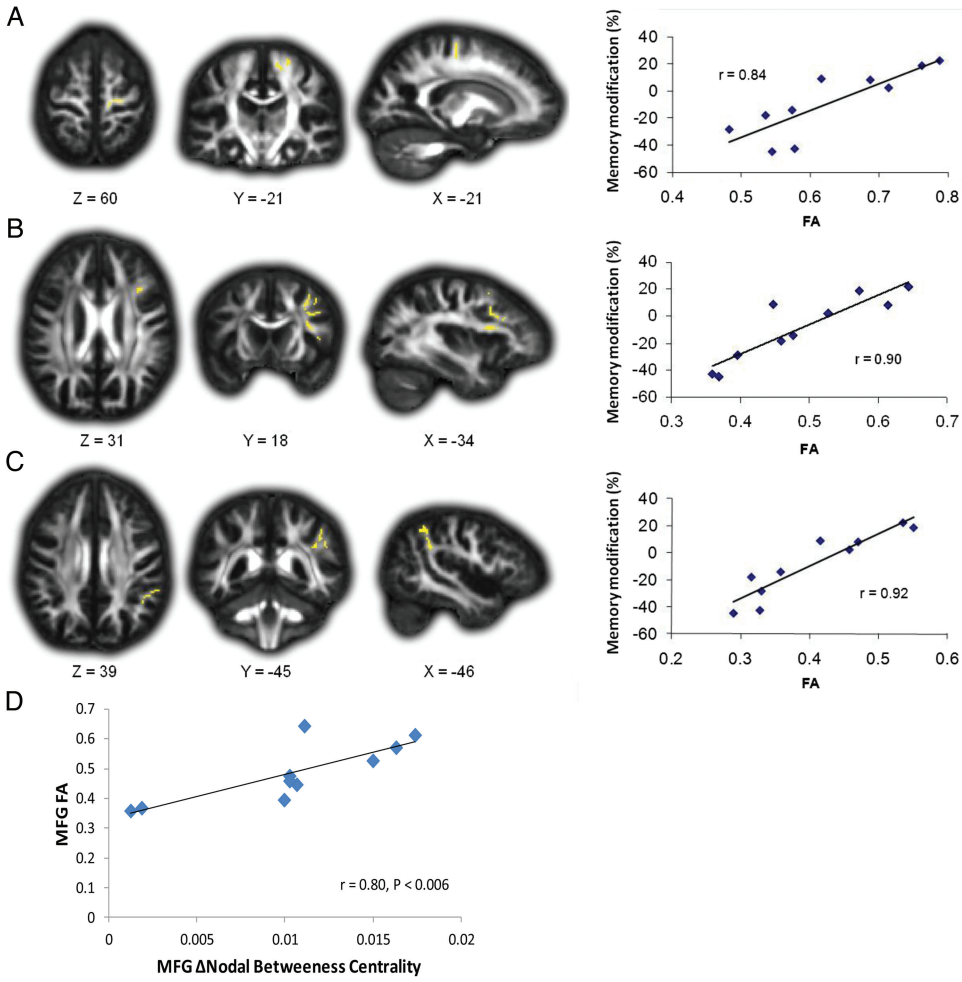

Figure 5. Memory modification correlated with WM FA in 3 contralesional WM regions, in the vicinity of the (*A*) precentral gyrus, (*B*) middle-frontal gyrus (MFG), and (*C*) anterior intraparietal area (AIP). Correlation clusters are shown in yellow. MNI coordinates indicate the center-of-mass of each cluster. Scatter plots depict the correlation for each cluster. Voxel-wise statistical images were thresholded at $P < 0.05$ (FDR corrected, see Methods). (*D*) Nodal betweenness centrality in the contralesional MFG correlated with FA in the same region.

et al. 2010). Therefore, together with the results here, this may suggest that the role of M1 and its connecting fibers is important after a memory is initially consolidated and requires further fine-tuning to translate into efficient motor function. This notion is consistent with the framework according to which as motor learning progresses, activity is shifted from anterior to more posterior parts of the brain since the core motor network becomes more involved in automatic fine-tuning of motor function, and there is less reliance on prefrontal executive and attentional resources (Hikosaka et al. 2002; Dayan and Cohen 2011). The association of memory modification with altered contralesional structures homologous to the damaged WM pathways may be related to poststroke structural plasticity mechanisms, which could be tested by future longitudinal studies.

Comparing the reactivation and no-reactivation conditions, significant transfer was observed for the training sessions and marginally significant transfer for the test sessions. It appears that these effects were driven by transfer in the control group. These transfer effects, even if not significant between groups, can affect the interpretation of the present data and may present a confounding factor that should be taken into account. Therefore, the no-reactivation condition could correspond to an extension/transfer of what participants had initially learned, representing a later learning stage. In addition, the nonsignificant between-group differences in transfer effects could be attributed to a lack of power. In the context of memory modification, it is therefore conceivable that the patients' impairments in modification of the original memory carried over to result in less-efficient transfer effects compared with healthy controls. Thus, if the experiment with a new sequence does not represent new learning but rather extension of the original learning, this extension could also be less efficient in patients due to their impaired ability to modify the memory. Of note, the results showing that performance on an untrained sequence was not significantly different from the performance reached at the end of the training session on Day 1, that is, after 9 trials of practice, provides another indication of potential transfer effects between sequences.

Interestingly, dissociable mechanisms underlying consolidation and memory modification through reconsolidation have been suggested at the cellular level as well (Lee et al. 2004; Dudai 2012). When studying processes that result in the modification of memory strength following its reactivation, evidence from animal studies showing different conditions relevant for these processes should be taken into account. For example, it was shown that stronger memories involving more training are

generally more stable (Eisenberg et al. 2003; Wang et al. 2009). Therefore, in the context of our results, it is conceivable that patients did not create a strong enough memory to start with and that memory would have been better if more practice had been provided on Day 1 such that a stronger memory trace would have been formed prior to the sessions held on Days 2 and 3. Future studies should be specifically designed to address this open question. Accordingly, engagement of M1 and its cortical connections may relate to the level of memory stability achieved rather than to the memory mechanism itself. In the context of motor learning, the effects of hand dominance should also be further explored.

The results here suggest that consolidation and reconsolidation following memory reactivation can be looked upon as mechanistically different stages of learning. Altogether, these findings are consistent with an evolutionary framework, according to which information previously consolidated engages additional processes for successful improvement of the memory trace. Understanding of these processes is crucial to develop effective interventions to improve procedural learning and recovery of damaged skills following human neurological diseases. From a clinical point of view, our results of differences in stages of motor learning after stroke relative to age-matched controls raise the exciting opportunity to explore in the future if different intervals between reactivating events and different practice or reactivation sessions could optimize the patients' memory and learning stages relative to those in controls.

Supplementary Material

Supplementary material can be found at: http://www.cercor.oxfordjournals.org/.

Funding

This research was supported by the Intramural Research Program of the National Institute of Neurological Disorders and Stroke (NINDS), National Institutes of Health. N.C. was supported by the NINDS Ruth L. Kirschstein National Research Service Award (NRSA). E.R.B. was supported by the Center for Neuroscience and Regenerative Medicine (CNRM). K.N. was supported by the Canadian Institutes of Health Research (CIHR) and the Natural Sciences and Engineering Research Council (NSERC).

Notes

We thank Eran Dayan and Sunbin Song for valuable comments on earlier versions of this manuscript. We thank Mae Brooks and Rita Volochayev for their important role in patient recruitment.

References

Alberini CM. 2011. The role of reconsolidation and the dynamic process of long-term memory formation and storage. Front Behav Neurosci. 5:12.

Bazin PL, Ellingsen LM, Pham DL. 2007. Digital homeomorphisms in deformable registration. Inf Process Med Imaging. 20: 211–222.

Borra E, Belmalih A, Calzavara R, Gerbella M, Murata A, Rozzi S, Luppino G. 2008. Cortical connections of the macaque anterior intraparietal (AIP) area. Cereb Cortex. 18:1094–1111.

Buch ER, Modir Shanechi A, Fourkas AD, Weber C, Birbaumer N, Cohen LG. 2012. Parietofrontal integrity determines neural modulation associated with grasping imagery after stroke. Brain. 135:596–614.

Budde MD, Frank JA. 2010. Neurite beading is sufficient to decrease the apparent diffusion coefficient after ischemic stroke. Proc Natl Acad Sci USA. 107:14472–14477.

Celnik P, Paik NJ, Vandermeeren Y, Dimyan M, Cohen LG. 2009. Effects of combined peripheral nerve stimulation and brain polarization on performance of a motor sequence task after chronic stroke. Stroke. 40:1764–1771.

Censor N, Dayan E, Cohen LG. 2014a. Cortico-subcortical neuronal circuitry associated with reconsolidation of human procedural memories. Cortex. 58:281–288.

Censor N, Dimyan MA, Cohen LG. 2010. Modification of existing human motor memories is enabled by primary cortical processing during memory reactivation. Curr Biol. 20:1545–1549.

Censor N, Horovitz SG, Cohen LG. 2014b. Interference with existing memories alters offline intrinsic functional brain connectivity. Neuron. 81:69–76.

Dayan E, Cohen LG. 2011. Neuroplasticity subserving motor skill learning. Neuron. 72:443–454.

de Beukelaar TT, Woolley DG, Wenderoth N. 2014. Gone for 60 seconds: reactivation length determines motor memory degradation during reconsolidation. Cortex. 59:138–145.

Debiec J, LeDoux JE, Nader K. 2002. Cellular and systems reconsolidation in the hippocampus. Neuron. 36:527–538.

Dudai Y. 2012. The restless engram: consolidations never end. Annu Rev Neurosci. 35:227–247.

Duque J, Mazzocchio R, Stefan K, Hummel F, Olivier E, Cohen LG. 2008. Memory formation in the motor cortex ipsilateral to a training hand. Cereb Cortex. 18:1395–1406.

Eisenberg M, Kobilo T, Berman DE, Dudai Y. 2003. Stability of retrieved memory: inverse correlation with trace dominance. Science. 301:1102–1104.

Folstein MF, Folstein SE, McHugh PR. 1975. "Mini-mental state". A practical method for grading the cognitive state of patients for the clinician. J Psychiatr Res. 12:189–198.

Genovese CR, Lazar NA, Nichols T. 2002. Thresholding of statistical maps in functional neuroimaging using the false discovery rate. Neuroimage. 15:870–878.

Glickman S. 1961. Perseverative neural processes and consolidation of the memory trace. Psychol Bull. 58:218–233.

Hermundstad AM, Brown KS, Bassett DS, Carlson JM. 2011. Learning, memory, and the role of neural network architecture. PLoS Comput Biol. 7:1.

Hikosaka O, Nakamura K, Sakai K, Nakahara H. 2002. Central mechanisms of motor skill learning. Curr Opin Neurobiol. 12:217–222.

Kandel ER. 2001. The molecular biology of memory storage: a dialogue between genes and synapses. Science. 294:1030–1038.

Karni A, Meyer G, Jezzard P, Adams MM, Turner R, Ungerleider LG. 1995. Functional MRI evidence for adult motor cortex plasticity during motor skill learning. Nature. 377:155–158.

Korman M, Doyon J, Doljansky J, Carrier J, Dagan Y, Karni A. 2007. Daytime sleep condenses the time course of motor memory consolidation. Nat Neurosci. 10:1206–1213.

Kunimatsu A, Itoh D, Nakata Y, Kunimatsu N, Aoki S, Masutani Y, Abe O, Yoshida M, Minami M, Ohtomo K. 2007. Utilization of diffusion tensor tractography in combination with spatial normalization to assess involvement of the corticospinal tract in capsular/pericapsular stroke: feasibility and clinical implications. J Magn Reson Imaging. 26:1399–1404.

Lee JL. 2008. Memory reconsolidation mediates the strengthening of memories by additional learning. Nature Neurosci. 11:1264–1266.

Lee JL, Everitt BJ, Thomas KL. 2004. Independent cellular processes for hippocampal memory consolidation and reconsolidation. Science. 304:839–843.

Leemans A, Jones DK. 2009. The B-matrix must be rotated when correcting for subject motion in DTI data. Magn Reson Med. 61:1336–1349.

Monfils MH, Cowansage KK, Klann E, LeDoux JE. 2009. Extinction-reconsolidation boundaries: key to persistent attenuation of fear memories. Science. 324:951–955.

Mori S, Zhang J. 2006. Principles of diffusion tensor imaging and its applications to basic neuroscience research. Neuron. 51:527–539.

Nader K, Hardt OA. 2009. A single standard for memory: the case for reconsolidation. Nat Rev Neurosci. 10:224–234.

Nader K, Schafe GE, Le Doux JE. 2000. Fear memories require protein synthesis in the amygdala for reconsolidation after retrieval. Nature. 406:722–726.

Newton JM, Ward NS, Parker GJ, Deichmann R, Alexander DC, Friston KJ, Frackowiak RS. 2006. Non-invasive mapping of corticofugal fibres from multiple motor areas–relevance to stroke recovery. Brain. 129:1844–1858.

Pierpaoli C, Walker L, Irfanoglu MO, Barnett A, Basser P, Chang LC, Koay C, Pajevic S, Rohde G, Sarlls J, et al. 2010. TORTOISE: an integrated software package for processing of diffusion MRI data. ISMRM 18th annual meeting, Stockholm, Sweden, 1597.

Riley JD, Le V, Der-Yeghiaian L, See J, Newton JM, Ward NS, Cramer SC. 2011. Anatomy of stroke injury predicts gains from therapy. Stroke. 42:421–426.

Robertson EM, Press DZ, Pascual-Leone A. 2005. Off-line learning and the primary motor cortex. J Neurosci. 25:6372–6378.

Rohde GK, Barnett AS, Basser PJ, Marenco S, Pierpaoli C. 2004. Comprehensive approach for correction of motion and distortion in diffusion-weighted MRI. Magn Reson Med. 51:103–114.

Rubinov M, Sporns O. 2010. Complex network measures of brain connectivity: uses and interpretations. Neuroimage. 52: 1059–1069.

Sandrini M, Censor N, Mishoe J, Cohen LG. 2013. Causal role of prefrontal cortex in strengthening of episodic memories through reconsolidation. Curr Biol. 23:2181–2184.

Ungerleider LG, Doyon J, Karni A. 2002. Imaging brain plasticity during motor skill learning. Neurobiol Learn Mem. 78:553–564.

Walker MP, Brakefield T, Hobson JA, Stickgold R. 2003. Dissociable stages of human memory consolidation and reconsolidation. Nature. 425:616–620.

Wang SH, de Oliveira Alvares L, Nader K. 2009. Cellular and systems mechanisms of memory strength as a constraint on auditory fear reconsolidation. Nat Neurosci. 12:905–912.

Wu M, Chang LC, Walker L, Lemaitre H, Barnett AS, Marenco S, Pierpaoli C. 2008. Comparison of EPI distortion correction methods in diffusion tensor MRI using a novel framework. Med Image Comput Comput Assist Interv. 11:321–329.

Zhang H, Yushkevich PA, Alexander DC, Gee JC. 2006. Deformable registration of diffusion tensor MR images with explicit orientation optimization. Med Image Anal. 10:764–785.

Zhang Y, Zhang J, Oishi K, Faria AV, Jiang H, Li X, Akhter K, Rosa-Neto P, Pike GB, Evans A, et al. 2010. Atlas-guided tract reconstruction for automated and comprehensive examination of the white matter anatomy. Neuroimage. 52:1289–1301.